Point of Common Coupling Power Factor Conditioning of Connected Loads with PWM Rectifier

MOHAMED A. AHMED
Electrical Engineering Department
Jouf University, Faculty of Engineering, Saudi Arabia.
Benha University, Faculty of Engineering Egypt.
madel@ju.edu.sa

Abstract: - The proliferation of poor power factor loads can deteriorate the network due to their negative impacts. In this research, a power factor conditioning of PCC is presented as another role of pulse width modulation rectifier. The main purpose of PWM rectifier is to adjust and regulate the output DC-voltage with low harmonic distortion of AC-source current. If inductive loads connected to same PCC, the PWM rectifier can also compensate for load reactive power. These two functions of PWM rectifier can improve overall system power factor and decrease added cost elaborated with equipment required for compensation. The proposed control scheme is based on d-q theory in which transformation from abc to d-q frames is carried out for both load and converter currents. Quadrature portion of load current, which represents load reactive power, will be inserted in current controller with negative phase to compensate for reactive power and improve poor power factor. The proposed control algorithm is realized by a low-cost 80C196KC microcontroller which provides multi-functions adequate for practical system implementation. Inductive load emulation is presented by a three-phase induction motor due to its widespread applications and variable power factor at different mechanical loads.

Key-Words: - PWM rectifier, harmonics, inductive load, power factor, d-q theory, microcontroller

1 Introduction

Power factor exhibits a fundamental index for illustrating power quality and voltage stability in power system. It is well recognized that loads with poor power factor contribute to low voltage quality and increase losses in electric grid. In addition, it reduces grid transmission capacity, substation voltage stability, and can cause voltage breakdown at large load [1- 4]. On the other hand, a relatively little correction in power factor can achieve a significant reduction in system power losses and enhance grid voltage stability and power quality.

Nowadays, active PWM rectifier has a widespread usage in AC/DC conversion according to its different characteristics, such as stabilization of DC-link voltage, bi-directional power flow, harmonic free line current, and displacement factor control [5- 10]. The topology of PWM rectifier, presented in figure 1, shows that it consists of three legs VSI that has its DC-side linked to a smoothing capacitor and AC-side coupled to grid through three-line inductors. This topology enables PWM rectifier to control reactive power alongside its AC/DC conversion. Different control strategies are proposed to operate the PWM rectifier [11-22].

In this paper, a lightly loaded three-phase induction motor (i.e. poor power factor inductive load) is connected to same PCC of PWM rectifier to test the system performance. The reactive components of motor current (iq) is extracted by d-q theory and then added with negative sign to current control loop of PWM rectifier.

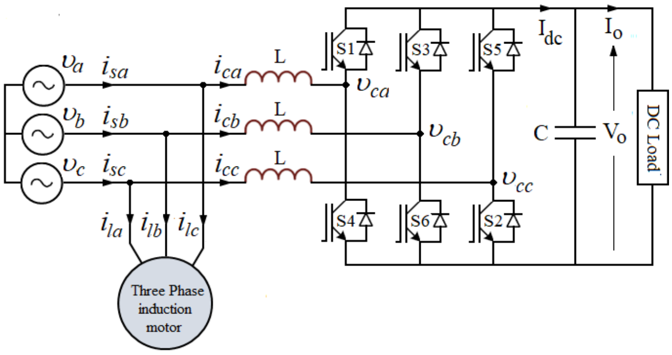

Fig. 1. PWM rectifier and induction motor at same PCC.

In this context, the converter circuit operates as synchronous condenser to generate reactive power demanded by the motor and hence improves overall system power factor.

The switching method of VSI power circuit is functioned by using PWM hysteresis current control scheme. This scheme has the advantages of straightforwardness in algorithm and perfect spectral performance of line current [23- 27].

2 Theory and Operation

The power circuit of three-phase PWM rectifier in VSI bridge connection is shown in figure 1. In this topology, the DC-link voltage (Vdc) should be controlled as in (1) to emphasize linear PWM operation and steady sinusoidal mains current [28].

$$V_{dc} \geq \frac{2\sqrt{2}}{\sqrt{3}} V_{LL} \tag{1}$$

where; V_{LL} is rms line to line supply voltage.

The circuit shown in figure 2 explains the operation of PWM rectifier, where it represents a single-phase equivalent circuit of PWM rectifier system shown in figure 1. In addition, the phasor diagram of overall system is shown in figure 3. The converter voltage vector (V_{ca}) is used to adjust the phase angle (θ_s) of ac line current (I_{sa}). For unity power factor operation, the magnitude and phase angle of converter voltage is controlled so that θ_s equal zero, and the switching pattern of converter IGBTs emphasizes sinusoidal current waveform. In this manner, the PWM rectifier power circuit delivers the motor reactive power instead of utility mains.

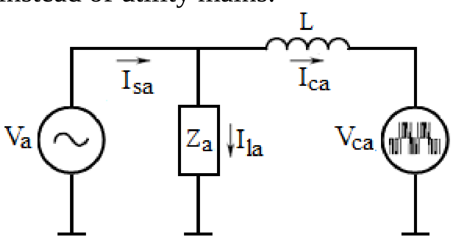

Fig. 2. Single line diagram of the system.

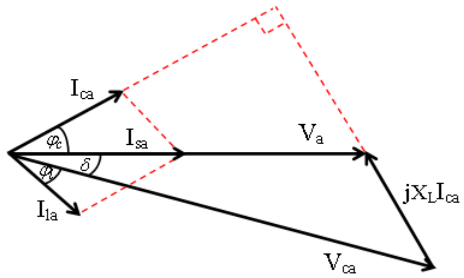

Fig. 3. Phasor diagram of the system.

where; δ is the converter voltage angle, φ_c is th e converter current angle, and φ_l is the load Referring to figure 1, equations representing the power circuit are:

$$\begin{bmatrix} i_{sa} \\ i_{sb} \\ i_{sc} \end{bmatrix} = \begin{bmatrix} i_{la} \\ i_{lb} \\ i_{lc} \end{bmatrix} + \begin{bmatrix} i_{ca} \\ i_{cb} \\ i_{cc} \end{bmatrix} \tag{2}$$

$$\begin{bmatrix} L\frac{d}{dt} i_{ca} \\ L\frac{d}{dt} i_{cb} \\ L\frac{d}{dt} i_{cc} \end{bmatrix} = V_{dc} \begin{bmatrix} \frac{-2}{3} & 1 & 1 \\ 1 & \frac{-2}{3} & 1 \\ 1 & 1 & \frac{-2}{3} \end{bmatrix} \begin{bmatrix} S_1 \\ S_3 \\ S_5 \end{bmatrix} + \begin{bmatrix} \upsilon_a \\ \upsilon_b \\ \upsilon_c \end{bmatrix} \tag{3}$$

$$\frac{dV_{dc}}{dt} = \frac{1}{C}\left(I_{dc}\text{-}I_o\right) \tag{4}$$

$$I_{dc} = S_1 I_{ca} + S_3 I_{cb} + S_5 I_{cc} \tag{5}$$

where S_1, S_3, S_5 are the status (0 or 1) of upper switches.

3 Proposed Control Scheme

There are two main purposes of converter controller; the first one is to eliminate supply current harmonic components, while the second purpose is to adjust and regulate DC output voltage. Additionally, the controller can also compensate for reactive current absorbed by the inductive load. These two functions are accomplished by applying *abc-dq* transformation for both load current and converter current. It is well known that the direct current (i_d) represents the active power, while the quadrature current component (i_q) represents reactive power. By eliminating harmonic and reactive power components from line current, it appears sinusoidal and has almost zero displacement angle. Thus, overall system acts as resistive load and enhance grid power quality.

According to three-phase three-wire system topology, the zero-sequence current is eliminated and *d-q* transformation may be expressed as;

$$K = \frac{2}{3}\begin{bmatrix} \cos(\theta) & \cos(\theta\text{-}\frac{2}{3}) & \cos(\theta+\frac{2}{3}) \\ \text{-}\sin(\theta) & \text{-}\sin(\theta\text{-}\frac{2}{3}) & \text{-}\sin(\theta+\frac{2}{3}) \end{bmatrix} \tag{6}$$

where; K is the coefficient of transformation, and θ is the instantaneous angle of an arbitrary frequency.

Direct and quadrature components of load current (i_{l_dq}) and converter current (i_{c_dq}) can be obtained by applying the transformation of equation (6) according to;

$$i_{l\_dq} = K i_{l\_abc} \tag{7}$$

$$i_{c\_dq} = K i_{c\_abc} \tag{8}$$

Both direct and quadrature components of converter current (i_{c_d}, i_{c_q}) contain DC and AC components as;

$$i_{c\_d} = \bar{i}_{c\_d} + \tilde{i}_{c\_d} \tag{9}$$

$$i_{c\_q} = \bar{i}_{c\_q} + \tilde{i}_{c\_q} \tag{10}$$

Figure 4 presents the block diagram of proposed control system. In this controller, the DC output voltage is regulated by PI controller, while the reference signal of direct converter current ($i^*_{c\_d}$) is generated by adding the DC components of direct converter current ($\bar{i}_{c\_d}$) to PI controller output. In addition, to compensate for load reactive power, the negative value of quadrature components of load current ($-i_{l\_q}$) is considered the reference quadrature components of converter current ($i^*_{c\_q}$).

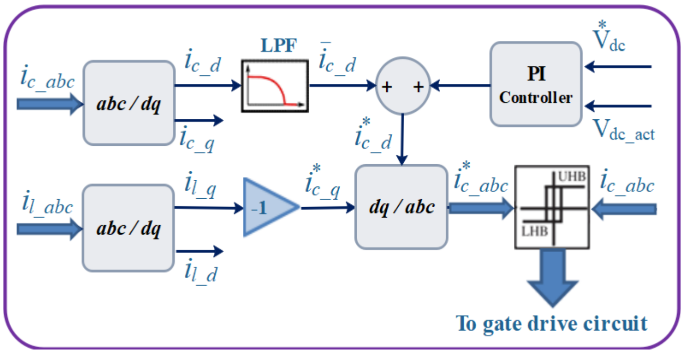

Fig. 4. Blok diagram of proposed control strategy.

4 Simulation Results

A MATLAB/Simulink is used to build the proposed simulation platform to evaluate system performance under different operating conditions as shown in figure 5.

According to equation (1), the DC output voltage is designed to be 700V for better PWM switching performance. A lightly loaded three phase induction motor with a low PF of 0.66 is shunted to PCC. Table I exhibits overall system parameters.

Table 1. System Parameters

Parameter	Value
Line voltage	V_{LL}=380V
DC output voltage	$V_{dc\text{-}ref}$ =700V
filer inductor	L=5mH
PWM rectifier load	R_{load}=50Ω
Filter capacitor	C=1000μF
Induction motor	10 hp, 380V, 50Hz, 90% efficiency, and 0.66 PF at light load.

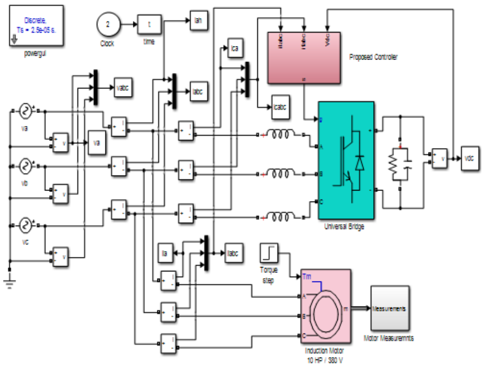

Fig. 5. MATLAB/Simulink model of proposed PWM rectifier system.

Figure. 6 presents the motor line current (i_{la}) at steady state with respect to the source voltage (υ_{sa}) and its associated active (P_l) and reactive (Q_l) powers.

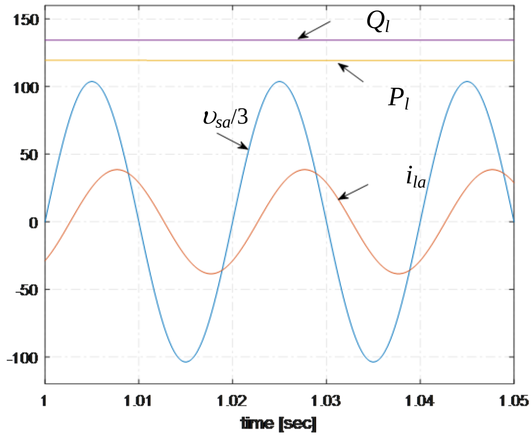

Fig. 6. Induction motor current and its associated powers.

The performance of PWM rectifier system is shown in figure 7 according to proposed controller. The figure exhibits that the source current i_{sa} is almost sinusoidal and with the same phase of source voltage υ_{sa}. In addition, the output voltage V_{DC} is adjusted to its predefined value of 700V.

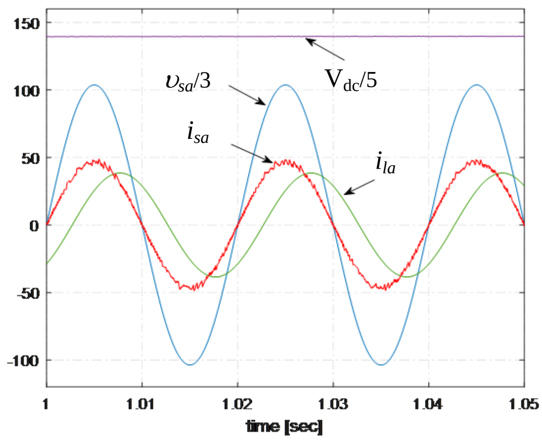

Fig. 7. Performance of PWM rectifier system.

The spectrum of line current is shown in figure 8 as percent of its fundamental component. A low value of current THD (2.97%) is obtained.

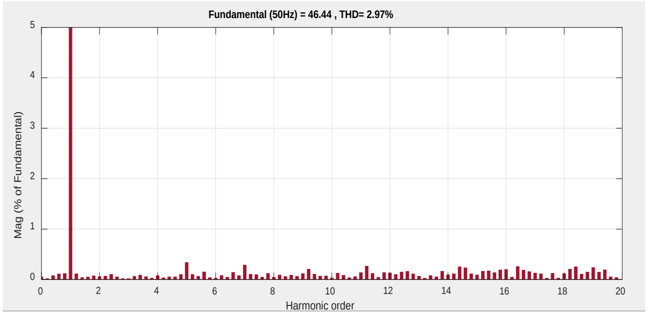

Fig. 8. Harmonic spectrum of line current.

Figure. 9 shows converter line current (i_{ca}) and its associated active and reactive powers (P_c, and Q_c). It also shows supply active and reactive powers (P_s, and Q_s) with respect to the source phase voltage. It can be noticed that converter current (i_{ca}) leads the source voltage with angle (φ_c), thus reactive power absorbed by motor is delivered from converter circuit rather than the source. In this situation, the source reactive power equals zero and converter reactive power is the negative value of motor reactive power ($-Q_c= Q_l$).

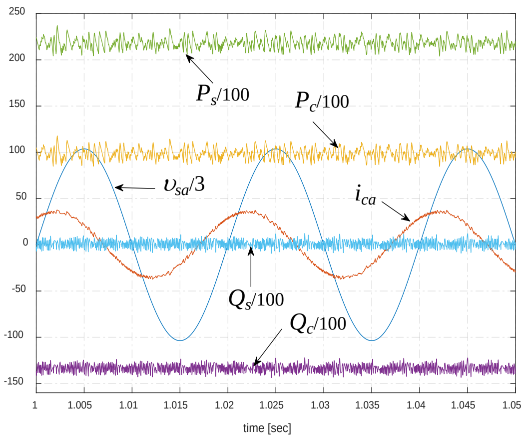

Fig. 9. System active and reactive powers.

The converter voltage (υ_{ca}) and its fundamental components (υ_{ca1}) are shown in figure 10 with respect to phase voltage. Referring to phasor diagram of figure 3, the waveform of υ_{ca1} lags the phase voltage with an angle (δ) to verify unity power factor operation.

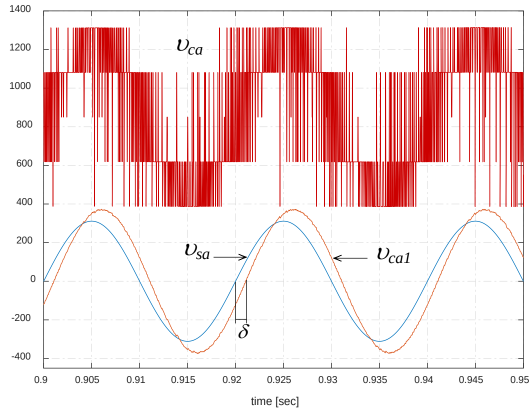

Fig. 10. Converter phase voltage and its fundamental components with respect to source voltage.

In figure 11, system quadrature currents and source direct current are presented. For lagging displacement factor of motor current, the quadrature component is negative (i_{lq}) and this current is compensated by the same positive value generated by the converter current (i_{cq}). Hence the quadrature source current (i_{sq}) has zero value, which indicates zero reactive power delivered by source voltage.

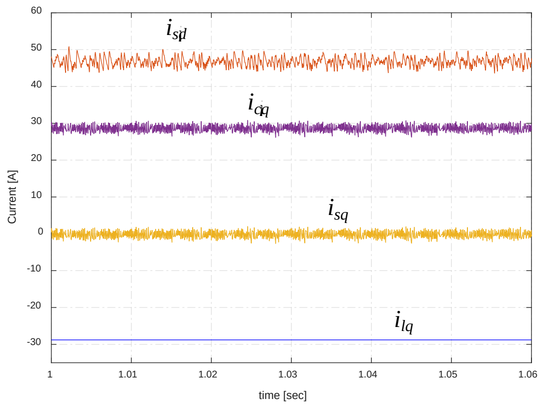

Fig. 11. Quadrature components of system currents.

Figure. 12 presents the response of PWM rectifier according to 18.75% step change in DC reference voltage. It is seen that the response of DC voltage to a sudden change in its reference value has a fast response (within a quarter cycle). In addition, the reactive power compensation effectively functioned where ($-i_{cq} = i_{lq}$) and (i_{sq}= *zero*).

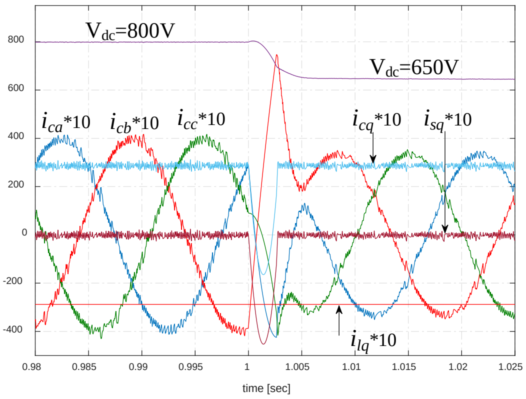

Fig. 12. Transient response of PWM rectifier according to step change in DC output voltage.

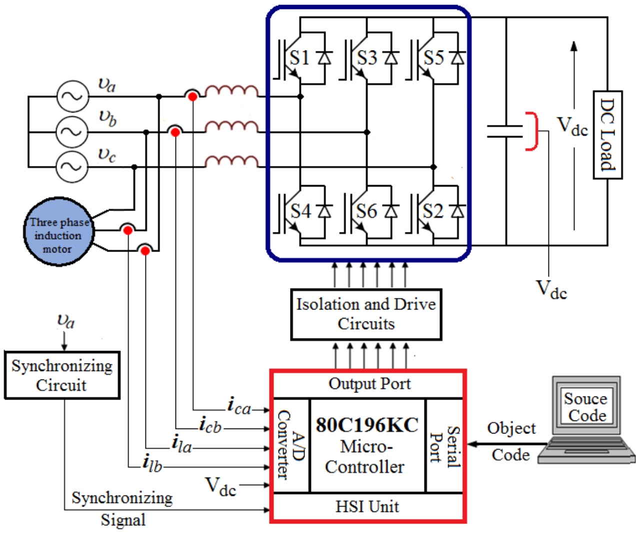

Fig. 13. Setup of experimental prototype.

5 Experimental Setup and Results

The prototype of three-phase PWM rectifier system is presented in figure 13. This system requires four current sensors, two of them required for measuring motor currents and the others for converter currents. In addition, a voltage sensor is required for measuring the DC output voltage. Thus, the selected microcontroller should have at least five A/D converter channels to adopt these measurements.

The proposed algorithm is carried out using a high speed 80C196KC microcontroller, and software code is written by assembly machine language to maximize the performance of microcontroller. Operation of PWM rectifier requires a synchronization between control circuit and AC power frequency. This function is accomplished by generating a square wave at power frequency and capturing its rising edges using the speed input unit (HSI). This unit is built in microcontroller. A unity sine-wave is generated each rising edge of synchronizing signal to provide PLL circuit. In addition, five A/D channels are used for reading measured current and voltage signals, whereas the switching signals required by IGBT's drive circuit are generated by digital output ports of microcontroller. According to large no. of A/D channels used, the lowest sample time can be obtained is 200µs. In practical experiments, a lightly loaded, 1-hp, three-phase induction motor is connected to PCC to realize a poor power factor inductive load.

Figure. 14 shows the waveform of line current with respect to phase voltage according to conventional three-phase diode bridge rectifier. The line current waveform is highly distorted and draws reactive power components. Figure. 15 presents the harmonic spectrum of line current, which determines that current waveform is highly distorted and has THD value of 22%.

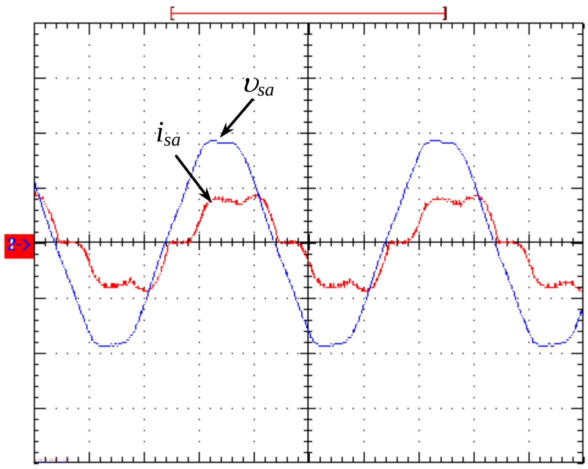

I [4A/div.], V_s [50V/div.], t [5ms/div.]

Fig. 14. Steady state performance of three-phase bridge diode rectifier.

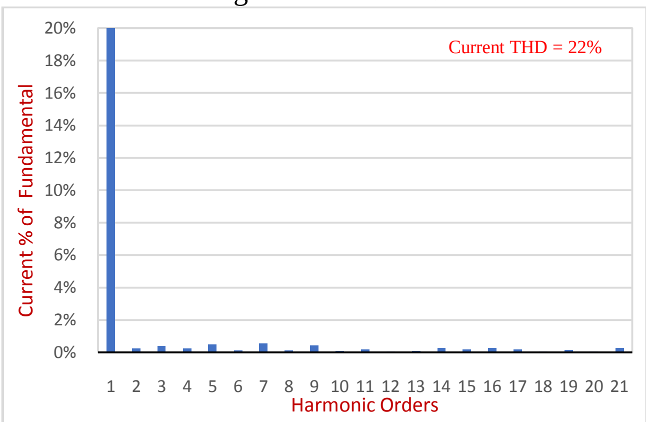

Fig. 15. Harmonic spectrum of line current drawn by three-phase bridge diode rectifier

Figure. 16 shows the performance of the PWM rectifier without connecting the motor as inductive load. The line current appears sinusoidal with a low THD value of 2.6% as indicated in figure 17. The dc output voltage is regulated at its predetermined value of 180V.

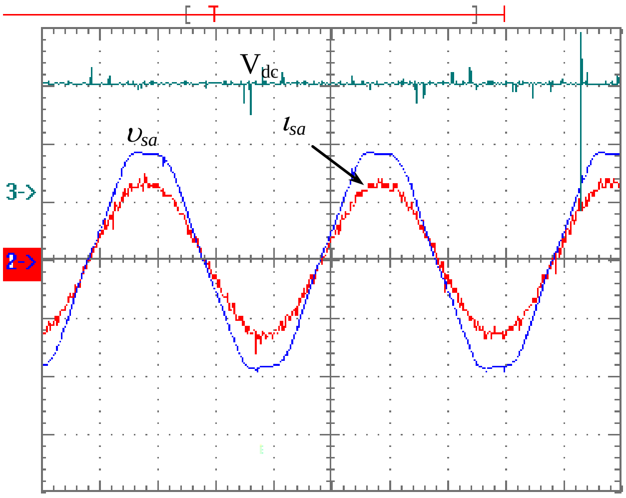

I [4A/div.], V_s [50V/div.], V_{dc} [100V/div.] t [5ms/div.]

Fig.17. Steady state performance of PWM rectifier.

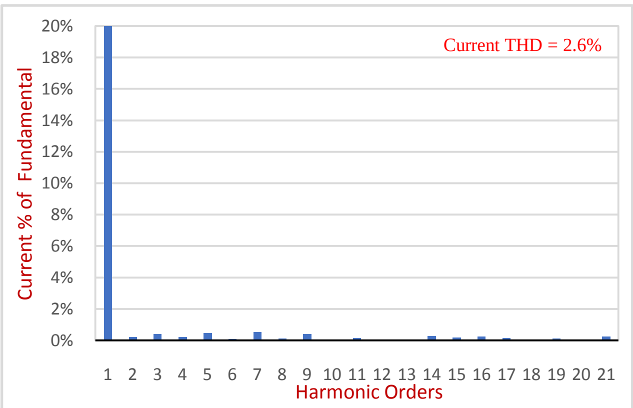

Fig. 17. Harmonic spectrum of line current drawn by three-phase PWM rectifier

Figure. 18 presents the three phase motor currents with respect to mains phase voltage. It can be observed that motor current lags the phase voltage with a relatively large angle, which indicates the poor power factor of motor operation especially when driving low mechanical loads.

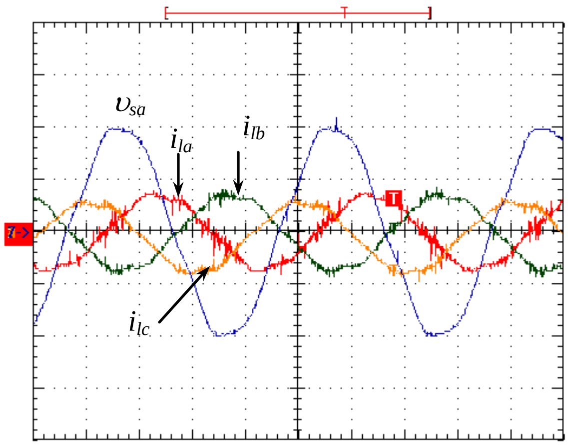

I [4A/div.], V_s [50V/div.], t [5ms/div.]

Fig. 18. Three-phase motor line currents and source voltage.

The performance of the PWM rectifier with function of reactive power compensation is shown in figure 19. It is seen that the three-phase line currents are near sinusoidal and in phase with supply voltage, which indicates that overall power factor is near unity. Thus, function of reactive power compensation is effectively operating. In addition, DC output voltage is regulated at its reference value of 180V.

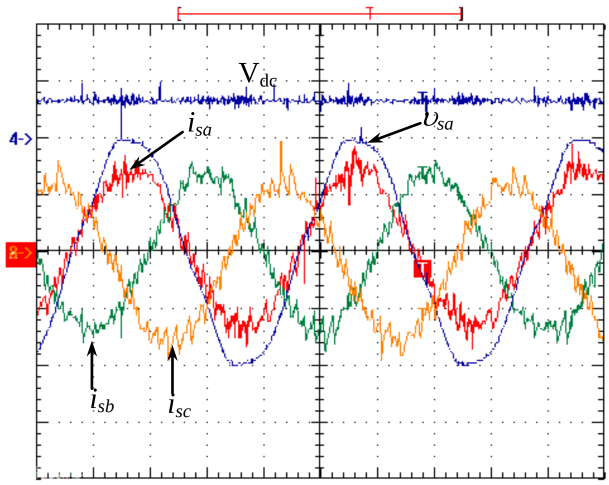

I [2A/div.], V_s [50V/div.], V_{dc} [300V/div.] t [5ms/div.]

Fig. 19. Performance of PWM rectifier according to reactive power compensations.

Figure 20 present the harmonic spectrum of supply current after harmonics and power factor compensation. The mains current has a low THD value of 4.23%, which meats the international harmonic standards.

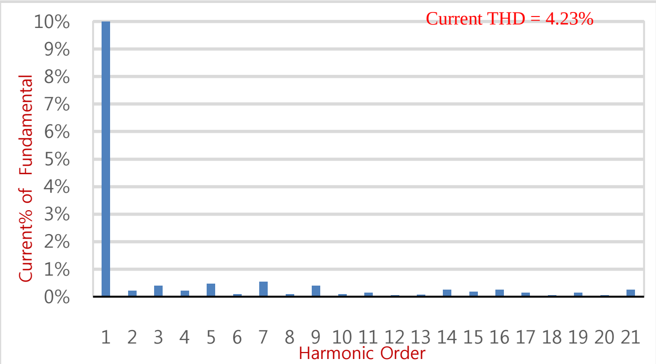

Fig. 20. Harmonic spectrum of mains current.

6 Conclusion

This paper proposes a power factor compensation as an additional function of PWM rectifier for low power factor inductive loads such as three phase induction motors connected to same PCC. The proposed control strategy is based on application of *dq* theory for both load current and converter current to compensate for low loads displacement factor and line current harmonics. A PI-controller is used to adjust and regulate the DC output voltage, while an LPF is used to extract the harmonic contents from direct components of line current. The control algorithm is accomplished by a single-chip low-cost 80C196KC microcontroller, by which software program is written in assembly language to maximize controller performance. The lowest sampling time obtained is 200μs which gives an approximated average switching frequency of 1KHz. The simulation and experimental results are taken at different operating condition to prove effectively that PWM converter delivers reactive power required by induction motor rather than supply and waveform of line current is near sinusoidal with low THD value of 4.23%.

References:

[1] B. Singh ; A. Saxena, D.P. Kothari, "Power factor correction and load balancing in three-phase distribution systems," Proceedings of IEEE TENCON '98, pp. 479 - 488, December 1998.

[2] U. Celtekligil, "Capacitive power factor and power quality correction of a light rail transportation system," 2008 50th International Symposium ELMAR, Zadar, pp. 415-418, Sept. 2008.

[3] W. G. Morsi and M. E. El-Hawary, "A new fuzzy-wavelet based representative quality power factor for stationary and nonstationary power quality disturbances," 2009 IEEE Power & Energy Society General Meeting, Calgary, AB, pp. 1-7, July 2009.

[4] L. Lin, J. Wang and W. Gao, "Effect of Load Power Factor on Voltage Stability of Distribution Substation," 2012 IEEE Power and Energy Society General Meeting, San Diego, CA, pp. 1-4., Nov. 2012.

[5] T. Shimizu ; T. Fujita ; G. Kimura ; J. Hirose, "A unity power factor PWM rectifier with DC ripple compensation," IEEE Transactions on Industrial Electronics, Vol. 44, No. 4, pp. 447 - 455, August 1997.

[6] M. P. Kazmierkowski and L. Malesani, "Current control techniques for three-phase voltage-source PWM converters: a survey," IEEE Transactions on Industrial Electronics, Vol. 45, No. 5, pp. 691-703, Oct. 1998.

[7] Bor-Ren Lin, "Analysis and implementation of a three-level PWM rectifier/inverter," IEEE Transactions on Aerospace and Electronic Systems, Vol. 36, No. 3, pp. 948 - 956, July 2000.

[8] J. Kikuchi, T.A. Lipo, "Three-phase PWM boost-buck rectifiers with power-regenerating capability," IEEE Transactions on Industry Applications, Vol. 38, No. 5, pp. 1361 - 1369, September 2002.

[9] Hyunjae Yoo, Jang-Hwan Kim, Seung-Ki Sul, "Sensorless Operation of a PWM Rectifier for a Distributed Generation," IEEE Transactions on Power Electronics, Vol. 22, No. 3, pp. 1014 - 1018, May 2007.

[10] M. A. Ahmed, S. A. Zaid, O. A. Mahgoub, "An Improved Performance for Three Phase Active Power Filter Based on Indirect Current Control Strategy", JPE, Journal of Power Electronics, Vol.6, No. 19, pp. 931-937, 2011.

[11] M. Malinowski ; M.P. Kazmierkowski ; A.M. Trzynadlowski, "A comparative study of control techniques for PWM rectifiers in AC adjustable speed drives," IEEE Transactions on Power Electronics, Vol. 18, No. 6, pp. 1390 - 1396, November 2003.

[12] R.Guedouani, B.Fiala, E.M. Berkouk, M.S. Boucherit, "Control of Three-Phase Pulse Width Modulation Voltage Rectifier," Proceedings of the 6th WSEAS/IASME Int. Conf. on Electric Power Systems, High Voltages, Electric Machines, Tenerife, Spain, PP. 246-251, December 16-18, 2006.

[13] Zixin Li, Yaohua Li, Ping Wang, Haibin Zhu, Congwei Liu, Wei Xu, "Control of Three-Phase Boost-Type PWM Rectifier in Stationary Frame Under Unbalanced Input Voltage," IEEE Transactions on Power Electronics, Vol. 25, No. 10, pp. 2521 – 2530, October 2010.

[14] Akira Sato, Toshihiko Noguchi, “Voltage-Source PWM Rectifier–Inverter Based on Direct Power Control and Its Operation Characteristics,” IEEE Transactions on Power Electronics, Vol. 26, No. 5, pp. 1559 - 1567, May 2011.
[15] A.Fekik, H. Denoun, N.Benamrouche, N. Beyahia, M.Zaouia, S.Haddad, “Comparative study of PI and FUZZY DC-voltage control for Voltage Oriented Control-PWM rectifier,” Proceedings of the 14th International Conference on Circuits, Systems, Electronics, Control & Signal Processing, Konya, Turkey, pp. 103-109, May 2015.
[16] Y. Zhang, C. Qu and J. Gao, "Performance Improvement of Direct Power Control of PWM Rectifier Under Unbalanced Network," in IEEE Transactions on Power Electronics, Vol. 32, No. 3, pp. 2319-2328, March 2017.
[17] Y. Cho and K. B. Lee, "Virtual-Flux-Based Predictive Direct Power Control of Three-Phase PWM Rectifiers with Fast Dynamic Response," in IEEE Transactions on Power Electronics, Vol. 31, No. 4, pp. 3348-3359, April 2016.
[18] Y. Zhang, J. Liu, J. Gao and H. Yang, "Direct power control of PWM rectifier with elimination of DC voltage oscillations and current harmonics under unbalanced network," 2017 IEEE Energy Conversion Congress and Exposition (ECCE), Cincinnati, OH, pp. 3405-3409, 2017.
[19] Y. Cho and K. B. Lee, "Virtual-flux-based power predictive control of three-phase PWM rectifiers using space-vector modulation," 2014 IEEE Energy Conversion Congress and Exposition (ECCE), Pittsburgh, PA, pp. 993-998, 2014.
[20] P. Dai, S. Dong, X. Fu and Y. Li, "Vector control of PWM rectifier based on a novel virtual flux observer," 2011 IEEE International Conference on Mechatronics and Automation, Beijing, pp. 1641-1645, 2011.
[21] B. D. Min, J. H. Youm and B. H. Kwon, "SVM-based hysteresis current controller for three-phase PWM rectifier," in IEE Proceedings - Electric Power Applications, vol. 146, no. 2, pp. 225-230, Mar 1999.
[22] Chong Zhu, Zhiyong Zeng, and Rongxiang Zhao, “Performance Analysis and Comparison of Post-Fault PWM Rectifiers Using Various Space Vector Modulation Methods,” Journal of Power Electronics, Vol. 16, No. 6, pp. 2258-2271, Nov. 2016.
[23] Tae-Won Chun, Meong-Kyu Choi, “Development of adaptive hysteresis band current control strategy of PWM inverter with constant switching frequency,” Proceedings of Applied Power Electronics Conference. APEC '96, pp. 194 - 199, March 1996.
[24] K.M. Rahman, M.R. Khan, M.A. Choudhury, M.A. Rahman, “Variable-band hysteresis current controllers for PWM voltage-source inverters,” IEEE Transactions on Power Electronics, Vol. 12, No. 6, pp. 964 - 970, November 1997.
[25] K.A. Corzine, “A hysteresis current-regulated control for multi-level drives,” IEEE Transactions on Energy Conversion, Vol. 15, No. 2, pp. 169 - 175, June 2000.

[26] Yukinori Kobayashi, Hirohito Funato, “Current control method based on hysteresis control suitable for single phase active filter with LC output filter,” 2008 13th International Power Electronics and Motion Control Conference, pp. 479 – 484, September 2008.

[27] Srinivas Pratapgiri, “Comparative analysis of Hysteresis Current Control and Direct Instantaneous Torque Control of Switched Reluctance Motor,” 2016 International Conference on Electrical, Electronics, and Optimization Techniques (ICEEOT), pp. 2856-2860, March 2016.

[28] N. Mohan, T.M. Undeland and W.P. Robbins, “Power Electronics: Converters, Applications and Design,” John Wiley & Sons, 2nd edition, pp.425-426, 1995.